Characterization of shallow geothermal energy installations through remote minute-resolved monitoring. A case study

García-Céspedes, J.,[1], Arnó, G.,[2], Herms, I.,[2], De Felipe, J.J.[3]

[1] Energía Coherente, C/ Nord 2 Bj.C, E-08004 Barcelona

[2] Àrea de Recursos Geològics, Institut Cartogràfic i Geològic de Catalunya (ICGC), Parc de Montjuïc s/n, 08038, Barcelona, Spain

[3] Departament of Mining, Industrial and ICT Engineering. Universitat Politècnica de Catalunya, Av/ Bases de Manresa 61, E-08242 Manresa. Barcelona. Spain

Jordi.garcia@energiacoherente.com

Keywords: Remote monitoring, Ground source heat pump, Partialisation losses, Seasonal performance, Part-load factor, Part-load ratio.

ABSTRACT

This work enlightens how remote monitoring of a shallow geothermal energy (SGE) system with minute-resolved data collection can contribute to the identification and quantification of efficiency-related problems. A specific SGE installation located in Tremp (Lleida, Spain), equipped with a vertical borehole heat exchanger (BHE) and a ground source heat pump (GSHP) was analyzed for this purpose. It was found a current average heating/cooling capacity over 10% under declared values of the GSHP equipment. In addition, the influence of part-load operation in seasonal performance was identified. The results were obtained from more than one complete year of data collection. The quality of the information obtained through data analysis was assessed in terms of the data-collection frequency. Weekly averaged data (available for more than 3 years) revealed that the capacity reduction is taking place progressively. Moreover, the seasonal coefficient of performance and seasonal energy efficiency ratio measured at the SGE installation under study were compared with those simulated by the software ground loop design (GLD, v2016). This supported the observations pointing to a progressive decay in performance.

1. INTRODUCTION

Low time-scale monitoring of SGE installations (sampling frequency below 1/hour) is an essential tool to create a precise picture of its performance. However, the convenience of implementing this tool is usually perceived as something related to the size of the facility. Above the domestic level (like in the case of central climatisation stations in residential and office buildings or district heating/cooling facilities), it is common to find a monitoring system installed along. Nevertheless, there is not yet any international standard addressing the monitoring and performance checking SGE installations from an integral perspective. The European standard EN15316 [EN 15316, 2017] includes a definition and system boundaries for Seasonal Performance Factor (SPF) calculation, but the measuring time-scale considered implicitly is large (seasonal). Besides, it can be found some initiatives concerning metering and monitoring protocols. These are motivated by national incentive programs [OFGEM, 2014], which require a technical approach for their implementation [OFGEM, 2019]. Traditionally, the quality and utility of existing monitoring systems have depended strongly on the good or bad praxis of the designers and installers. So far, the level of sophistication required for the monitoring systems has followed a diffuse cost-benefit criteria, due precisely to the lack of clear standards. In this sense, there has been some activity in the past years helping to address this issue [Normand R. et al., 2012; Sparn B. et al., 2013]. Probably the closest approach to a European standard on this topic is the European project SEPEMO, which aimed to set common metrics and system boundaries for seasonal performance assessment. Although up to date no new international standard has emerged from the results of SEPEMO project, its outcomes have been widely adopted by new projects where seasonal performance has been measured in hundreds of in-service SGE installations across Europe, generating high quality statistical data concerning heat pump technology and contributing to a rigorous benchmarking [Normand R.et al, 2010; Hughes D. 2018; Miara M. et al., 2017, Gehlin S.et al., 2018].

Nevertheless, the efforts made so far are focused on seasonal performance indicators from which certain operational aspects cannot be identified or quantified.

Part-load operation is an inherent source of performance degradation due to successive start-stop of the compressors, especially in heat pumps equipped with fixed-speed compressors. In this sense, the norm EN14825 [EN 14825, 2010] is the closest approach for the evaluation of seasonal performance under part-load conditions, although it is conceived from a laboratory environment test perspective. An analogous approach for in-service heat pumps operating under real conditions is still missing. Besides, in existing SGE installations, there are several factors apart from part-load operation that could introduce negative influence on the seasonal performance, like fouling formation in the inner walls of the pipes, brine/water leakage (leading to the presence of air bubbles in the heat exchanger circuits), refrigerant leakage or valve malfunctioning, among others.

Through the presentation of a particular case, this work aims to explore (and exploit) new capabilities of monitoring, data collection and processing for the analysis of small and middle-size SGE installations. Moreover, the barriers imposed by real operating conditions (non steady state dynamics) are delimited in order to conciliate the absence of laboratory conditions with an exhaustive characterisation, especially when part-load conditions take place.

Moreover, simulation of the case study by means of Ground Loop Design (GLD) software [Thermal Dynamics, 2016], will be used as an alternative tool to estimate the disagreement between the measured and expected performance of the SGE installation.

Nomenclature

COP	Coefficient of performance [-]
EER	Energy Efficiency ratio [-]
SCOP	Seasonal *COP* [-]
SEER	Seasonal *EER* [-]
PLF	Part-Load Factor [-]
PLR	Part-Load Ratio [-]
DHW	Domestic Hot Water
SV	Storage Vessel
E	Energy [kWh]
P	Power or heat rate [kW]
$\dot{\mathbf{Q}}$	Measured power or heat rate [kW]
$\dot{\mathbf{V}}$	Brine flow [m^3/min]
T	Temperature [ºC]
$\overline{\mathbf{T}}$	Mean Temperature ($T^{in} + T^{out}$)/2 [ºC]
c_p	Specific heat capacity [kJ/kgK]
ρ	Brine density [kg/m^3]
t	Time [min]

Subscripts

d	Declared
evap	At the evaporator
cond	At the condenser
comp	Concerning the compressor(s)
pump	Concerning the circulating pump (s)
ON	Compressor(s) ON
OFF	Compressor(s) OFF
brine	Concerning heat exchanger liquid (ground source)
h	Concerning heat production
c	Concerning heat rejection (cooling)
t	Concerning total heat exchanged with the building
e	Concerning electric energy consumption
gr	Concerning ground

Superscripts

load	Concerning the demand side
in	At the entrance
out	At the exit
A	Concerning heat pump module / compressor A
B	Concerning heat pump module / compressor B

2. DESCRIPTION OF THE CASE STUDY

2.1. SGE installation

The SGE installation under analysis comprises a GSHP (model Fighter 1330-60, from the company Nibe Industrier AB, Sweden) coupled to a vertical borehole heat exchanger (BHE) field (10 boreholes with a depth of 140 m each). The heat pump is equipped with two fixed-speed compressor stages operating in parallel (not tandem) and has an overall nominal heating capacity of 60kW, although its performance is better represented through Table 1, where several performance data is provided by the manufacturer. It is worth to mention that these values were obtained following the norm EN255 [EN 255, 1998] (already obsolete and superseded by EN14511 [EN 14511, 2008]), where reference test conditions are defined by T_{evap}^{in} and T_{cond}^{out}. Furthermore, according to the user manual, the reference performance tests were carried out by the manufacturer using a brine flow of 10.0 m^3/h at the external circuit (28% ethanol) and a secondary fluid flow of 4.6 m^3/h in the internal circuit (pure water).

The declared coefficient of performance and declared energy efficiency ratio (COP_d and EER_d, respectively) are calculated values according to norm EN14511 (P_{pump} = 1.74 kW):

$$\mathbf{COP_d} = \frac{\mathbf{P_h}\left(\mathbf{T_{evap}^{in}}, \mathbf{T_{cond}^{out}}\right)}{\mathbf{P_{comp}}\left(\mathbf{T_{evap}^{in}}, \mathbf{T_{cond}^{out}}\right) + \mathbf{P_{pump}}} \quad [\mathbf{1}]$$

$$EER_d = \frac{P_c(T_{evap}^{in}, T_{cond}^{out})}{P_{comp}(T_{evap}^{in}, T_{cond}^{out}) + P_{pump}} \quad [2]$$

In the SGE installation under study, pure water is used both in the external and internal circuits. The system fully meets the cooling, heating and domestic hot water (DHW) demand of an office building in the city of Tremp (Lleida, Spain), with no back-up unit available. There is a storage vessel of 750 l capacity and a DHW vessel of 1000 l. The climatisation of the building is carried out via fan-coils and splits.

Table 1: Nominal performance values of P_h, P_c and P_e corresponding to several test conditions defined by T_{evap}^{in} and T_{cond}^{out}. The grey-shadowed columns correspond to calculated values.

T_{evap}^{in} (ºC)	T_{cond}^{in} (ºC)	T_{cond}^{out} (ºC)	P_h (kW)	P_c (kW)	P_{comp} (kW)	COP_d	EER_d
-5	34,5	45	50,9	35,6	15,3	2,99	2,09
0	34,5	45	58,6	42,6	16,0	3,30	2,40
5	34,5	45	67,0	50,2	16,8	3,62	2,71
10	23,8	35	80,6	65,0	15,7	4,63	3,73
10	34,5	45	76,7	59,1	17,7	3,96	3,05
10	45,2	55	73,2	53,0	20,2	3,34	2,42
10	55,8	65	70,0	46,7	23,2	2,80	1,87

2.2 Monitoring system and data collection

The monitoring system of the installation comprises a remarkable amount of parameters both at production and distribution levels like alarms and operating status, as well as measured parameters concerning mainly temperatures, energy, all of them being remotely accessible through a private web portal. Nevertheless, only a few of them are recorded periodically and useful from an analytical perspective, namely:

- E_h [kWh]: Resolution: 1 kWh (Accuracy < 0.6%)

- E_c [kWh]: Resolution: 1 kWh (Accuracy < 0.6%)

- E_{DHW} [kWh]: Resolution: 1 kWh (Accuracy < 0.6%)

- E_e [kWh]: Resolution: 0.02 kWh (Accuracy < 0.5%). It accounts uniquely for the compressors and circulation pump (in agreement with EN14511).

- T_{SV}^{out} [ºC]: Resolution: 0.1 ºC (Accuracy < 0.5ºC) Measured by a sensor placed in the outlet duct the storage vessel (bottom part).

- T_{brine}^{out} [ºC]: Resolution: 0.1 ºC (Accuracy < 0.5ºC)

- T_{brine}^{in} [ºC]: Resolution: 0.1 ºC (Accuracy < 0.5ºC)

- t_{ON} [min]: Resolution: 1 min. It provides separate readouts of both compressors (named A and B) inside the heat pump.

Through the web portal, it is possible to access to these parameters in the form of graphical information, but also as datasets downloadable in .csv format in four different manners:

- Yearly: weekly-averaged (WA) data from the last year (57 points per dataset).

- Monthly: daily-averaged (DA) data from the last month (37 points per dataset)

- Daily: 30 minute-averaged (30MA) data from the last day (48 points per dataset)

- Hourly: minute-resolved (MR) data from the last hour (60 points per dataset).

A data-logger routine had to be programmed from a remote computer in order to save datasets (.csv format) every hour for the MR data and every day for the 30MA data. WA data was collected manually. DA data was discarded for the analysis since it did not provide any relevant feature over the rest. The large amount of .csv files collected (almost $8 \cdot 10^4$ files per year in the case of MR data) were managed using Microsoft Excel (2007), where download and processing routines were programmed under Visual Basic environment.

3. RESULTS

3.1 Data exploitation

Calculation of SCOP and SEER (see Table 2), as well as non-instant COP and EER (over a day, week or month) is straightforward and involves E_h, E_c, E_{DHW} and E_e:

$$SCOP = \left.\frac{E_h + E_{DHW}}{E_e}\right|_{1\ year} \quad [3]$$

$$SEER = \left.\frac{E_c}{E_e}\right|_{1\ year} \quad [4]$$

Table 2. Thermal loads, Electric consumption and SCOP and SEER corresponding to 3 years of WA data collection.

Season (heating / cooling)	E_h+E_{DHW} (kWh)	E_c (kWh)	E_e (kWh)	SCOP / SEER
Sep2015-May2016	89619		27347	3.28
Jun2016-Sep2016		33369	10308	3.24
Oct2016-May2017	86158		26889	3.20
May2017-Oct2017		40026	13874	2.88
Oct2017-Jun2018	89882		29117	3.09
Jun2018-Oct2018		37035	12529	2.98

Figure 1 depicts the evolution of COP and EER throughout 3 complete cold seasons and 4 complete warm seasons, respectively (calculated according to

expressions [3] and [4] using 1 week as the integrating period). The linear fits provide an estimation of the average yearly decreasing rate, being 2.0% for COP and 3.8% for EER.

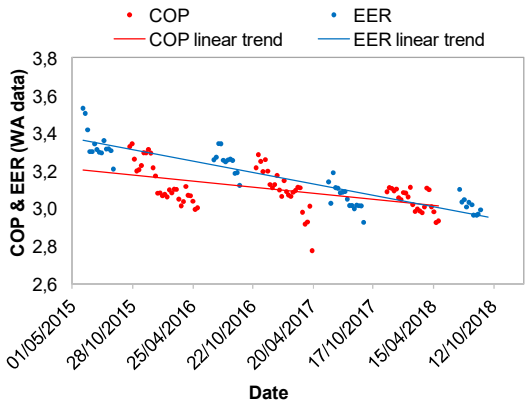

Figure 1. Time evolution of COP and EER from WA data. Values in the vicinity of a mode shift (heating to cooling or vice versa) have been suppressed to avoid distortion. Linear fit is shown to illustrate the decreasing trend along the years.

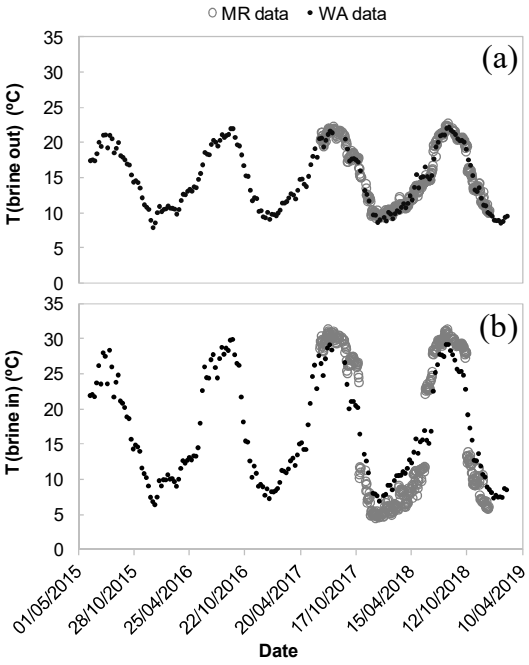

Figure 2. Time evolution of T_{brine}^{out} (top) and T_{brine}^{in} (bottom). WA data comprises a larger period of data than MR data because systematic collection of the latter started in June of 2017.

Concerning ground temperature evolution, T_{brine}^{out} provides the best picture. In Figure 2, the time evolution of T_{brine}^{out} and T_{brine}^{in} are presented, from WA and MR data. In the case of MR data, only the values of T_{brine}^{out} and T_{brine}^{in} during heat production or rejection are taken into consideration. Although this should cause no difference in WA and MR data for T_{brine}^{out} (as confirmed by Figure 2a) this is the reason why it a significant difference between WA data and MR data is observed in the case of T_{brine}^{in} (Figure 2b).

Energy exchanged with the ground can be evaluated just by using T_{brine}^{in}, T_{brine}^{out}. However, brine flow must be known:

$$\Delta E_{gr} = \int_0^{1\,year} \rho(\overline{T})\dot{V}(t)c_p(\overline{T})(T_{brine}^{out} - T_{brine}^{in})dt \cong$$

$$\cong \sum_i \rho(\overline{T})\dot{V}(t)c_p(\overline{T})\left(T_{brine}^{out} - T_{brine}^{in}\right)_i \Delta t_i \qquad [5]$$

Where Δt_i =1 min, $\forall i$ and $\overline{T}$ is taken as the mean value of T_{brine}^{out} and T_{brine}^{in} at time interval Δt_i.

Instant building load ($\dot{Q}_t^{load}$) can also be estimated through E_h, E_c, E_{DHW}, but special attention must be paid to the time scale. Over a day, the overall energy delivered or removed from the building divided by a daytime can be fairly assumed as the average building load of that day:

$$\overline{\dot{Q}}_t^{load}\Big|_{1\,day} = \overline{\dot{Q}}_t\Big|_{1\,day} = \frac{\Delta E_t}{24}\Big|_{1\,day} \qquad [6]$$

However, the same reasoning would not necessarily apply to periods around 1 hour or below. This is true especially for fixed-speed compressors, since the heat pump operates at maximum capacity when it is ON regardless of the load. The best approximation is obtained if both t_{ON} and t_{OFF} are known for a certain ON/OFF cycle (MR data is needed):

$$\overline{\dot{Q}}_t^{load}\Big|_{1\,cycle} = \overline{\dot{Q}}_t\Big|_{1\,cycle} = \frac{\Delta E_t}{t_{ON} + t_{OFF}} \qquad [7]$$

Nevertheless, to perform this calculation in a systematic way for all the datasets is impractical, because t_{ON} and t_{OFF} are stochastic variables, so $\overline{\dot{Q}}_t$ should be calculated "manually" for each period identified and delimited. A much simpler method consists of using the values of $\overline{\dot{Q}}_t(t)$ from 30MA data:

$$\overline{\dot{Q}}_t(t) = \frac{\Delta E_t}{0.5}\Big|_{\Delta t=0.5h} \qquad [8]$$

Empirically, it is observed that a smoothing of the $\overline{\dot{Q}}_t(t)$ curve provides a consistent representation of the building instant load (see Figure 3). The smoothing is carried out mathematically by averaging over 5 values (it means that $\overline{\dot{Q}}_t(t)$ is averaged over 2.5h at each t) around a particular time t_i:

$$\bar{\dot{Q}}_t^{load}(t_i) \approx \bar{\dot{Q}}_{t-smoothed}(t_i) = \frac{1}{5}\sum_{j=i-2}^{j=i+2} \bar{\dot{Q}}_t(t_j) \qquad [9]$$

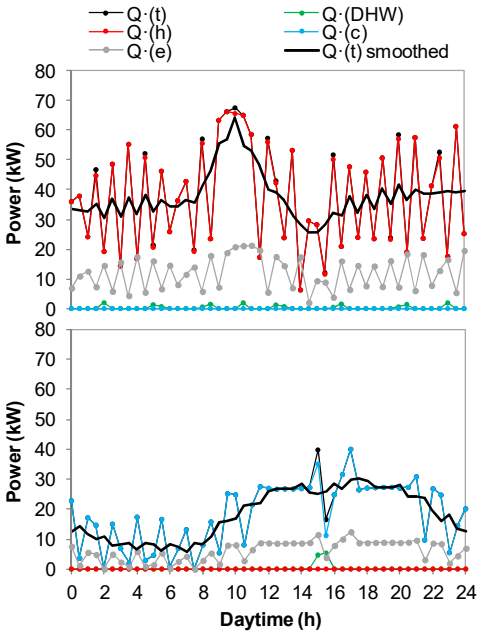

Figure 3. Capacity and electrical power rates calculated from 30MA data under heating mode (top plot, December 13th of 2017) and under cooling mode (bottom plot, July 13th of 2018). $\dot{Q}_{t-smoothed}$ is presented as an estimation of $\dot{Q}_t^{load}$.

Therefore, this method provides a reasonable estimation of the building load evolution with time and a fast identification of the peak loads in a certain month.

This is further confirmed by observing at the MR data corresponding to the time evolution of T_{brine}^{out}, T_{brine}^{in} and T_{SV}^{out}. From $\dot{Q}_{t-smoothed}$ curves, it can be identified quasi steady state time periods on the one hand from 1 a.m. to 6 a.m. and from 8 p.m. to 12 a.m. (December 13th of 2017, Figure 3, top); on the other hand from 3 a.m. to 7 a.m. and from 12 p.m. to 8 p.m. (July 13th of 2018, Figure 3, bottom). In Figure 4 the same time periods are characterised by a regular sequence of almost identical ON/OFF cycles, except for the period going from and from 12 p.m. to 8 p.m. on July 13th of 2018. In this last case, it is interesting to identify two periods with nearly constant T_{SV}^{out} (from 12 p.m. to 2 p.m. and from 6 p.m. to 8p.m.), which represent the situation when thermal load equals heat pump capacity (heat removal and heat supply rates coincide at the storage vessel). Although this is also an evidence of quasi steady state conditions, Figure 3 (bottom) aids a more accurate delimitation of the time period where such conditions take place.

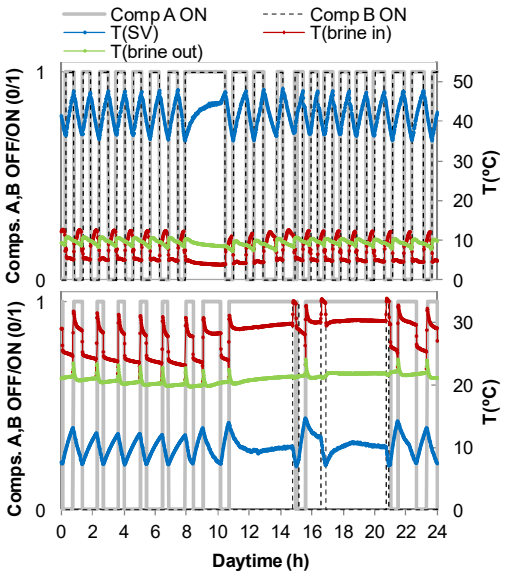

Figure 4. MR data corresponding to the parameters T_{brine}^{out}, T_{brine}^{in}, T_{SV}^{out}, recorded during December 13th of 2017 (top) and July 13th of 2018 (bottom). t_{ON} corresponding to both compressors A and B inside the heat pump are superimposed in all the plots (specified as "COMP A ON" and "COMP B ON" in the graphs).

One of the best tools for the characterisation of the GSHP under part-load conditions is the representation of the part-load factor (PLF) against the part-load ratio (PLR) [Corberán J. M. et al., 2013; Waddicor D.A. et al., 2016].

The PLR is the ratio between the thermal load and the heat pump capacity:

$$PLR = \frac{\dot{Q}_t^{load}}{\dot{Q}_t} \qquad [10]$$

When $\dot{Q}_t^{load}$ is constant or showing little variation (<10%) over time, quasi steady state conditions can be considered, and therefore expression [10] can be approximated [Corberán J. M. et al., 2013] as:

$$PLR = \frac{t_{ON}}{t_{ON} + t_{OFF}} \qquad [11]$$

Therefore, t_{ON} readout is required in combination with the identification of quasi steady state periods through $\dot{Q}_{t-smoothed}$.

Concerning the PLF, it is defined as the ratio between measured and declared COP or EER:

$$PLF_h = \frac{COP}{COP_d} \qquad [12]$$

$$PLF_c = \frac{EER}{EER_d} \qquad [12]$$

Expressions [11] and [12] are referred strictly to power ratios. However, under quasi steady state conditions, average power ratios can be approximated to the ratio of mean powers, but also to energy ratios, so it is valid to calculate the value of PLF for a certain period of time Δt (including cycling operation or not) according to:

$$PLF_h \cong \frac{COP|_{\Delta t}}{\left|\frac{1}{t_{ON}}\sum_{i=1}^{i=t_{ON}} COP_{d_i}\right|_{\Delta t}} \cong \cong \frac{\left.\frac{E_h}{E_e}\right|_{\Delta t}}{\left|\frac{1}{t_{ON}}\sum_{i=1}^{i=t_{ON}} \frac{P_h\left(T_{evap}^{in}, T_{cond}^{out}\right)_i}{P_{comp}\left(T_{evap}^{in}, T_{cond}^{out}\right)_i + P_{pump}}\right|_{\Delta t}} \quad [13]$$

$$PLF_c \cong \frac{EER|_{\Delta t}}{\left|\frac{1}{t_{ON}}\sum_{i=1}^{i=t_{ON}} EER_{d_i}\right|_{\Delta t}} \cong \cong \frac{\left.\frac{E_c}{E_e}\right|_{\Delta t}}{\left|\frac{1}{t_{ON}}\sum_{i=1}^{i=t_{ON}} \frac{P_c\left(T_{evap}^{in}, T_{cond}^{out}\right)_i}{P_{comp}\left(T_{evap}^{in}, T_{cond}^{out}\right)_i + P_{pump}}\right|_{\Delta t}} \quad [14]$$

Notice that for the calculation of PLF_h, only periods of heating were considered. It does not exclude the possibility of considering periods with DHW production, but for the sake of simplicity, it is preferable to distinguish between heating and DHW when calculating the PLF of a certain period.

In order to input P_h, P_c and P_e corresponding to each minute in expressions [13] and [14], it is necessary to know T_{evap}^{in} and T_{cond}^{out} to look up in the reference performance data (Table 1). However, since values in Table 1 are provided by the manufacturer as a set of discrete data, an interpolation function must be built-up first. Moreover, T_{evap}^{in} and T_{cond}^{out} are not parameters recorded by the monitoring system (although they are accessible in-situ at the heat pump equipment). Alternatively, it can be established the following equivalence for the particular case of the SGE installation under analysis:

$$T_{brine}^{out}|_{heating\ mode} \cong T_{evap}^{in} \cong T_{SV}^{out}|_{cooling\ mode} \quad [15]$$

$$T_{brine}^{in}|_{cooling\ mode} \cong T_{cond}^{out} \cong T_{SV}^{in}|_{heating\ mode} \quad [16]$$

Unfortunately, T_{SV}^{in} is neither recorded by the monitoring system, so there would be no physical means to get datasets representing T_{cond}^{out} under heating mode. To overcome this limitation, it is necessary to identify declared capacity and power in Table 1 by T_{evap}^{in} and T_{cond}^{in} instead of T_{evap}^{in} and T_{cond}^{out}, because T_{cond}^{in} can be identified with a recorded parameter:

$$T_{brine}^{out}|_{cooling\ mode} \cong T_{cond}^{in} \cong T_{SV}^{out}|_{heating\ mode} \quad [17]$$

This is the reason why there is an additional column in Table 1 showing the calculated T_{cond}^{in} values corresponding to each T_{cond}^{out}. T_{cond}^{in} is obtained from the following expression accounting for the declared capacity:

$$P_h\left(T_{evap}^{in}, T_{cond}^{out}\right) = \rho \dot{V}_{ref} c_p \left(T_{cond}^{out} - T_{cond}^{in}\right) \rightarrow$$

$$\rightarrow T_{cond}^{in} = T_{cond}^{out} - \frac{P_h\left(T_{evap}^{in}, T_{cond}^{out}\right)}{\rho \dot{V}_{ref} c_p} \quad [18]$$

Where $\dot{V}_{ref}$ is provided by the manufacturer as one of the test conditions required by norm EN255.

Figure 5 shows two collections of (PLR, PLF) values obtained from July-August of 2017 (cooling mode) and from December 2017 to January 2018 (heating mode). In both cases, it is observed that PLF decreases as the PLR approaches to 0.

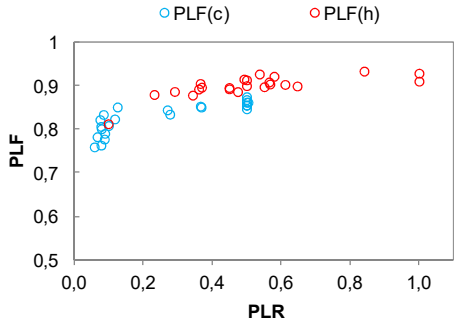

Figure 5. PLF obtained for a set of operating periods where quasi steady state conditions were identified, for cooling (blue dots) and heating (red dots) operating mode.

3.2 Simulation with GLD (v2016)

For the simulation of the SGE installation performance under the GLD software environment, it is necessary to have the information concerning three main blocks:

- BHE field characteristics. The geometry and the characteristics of the BHE field are defined by the ground characteristics, pipe geometry and materials, brine characteristics and circulation pump power consumption.

- Thermal loads. It is required to input the monthly thermal loads either for heating and cooling mode, along with the monthly peak load.

- Heat pump characteristics. GLD possesses a database with the declared performance data of several units from several manufacturers. Additionally, if the heat pump of the SGE installation under simulation is not among the list provided, it is possible to built a customized model in its *Edit/add heat pump* module (using values from Table 1 in this case). However the test conditions in the GLD modelling tool are referenced always to entering water temperatures (EWT), which means T_{evap}^{in} and T_{cond}^{in} instead of T_{evap}^{in} and T_{cond}^{out}. The reason for this relies on the fact that

American heat pump manufacturers follow ISO13256 [ISO 13256, 1998] as the standard for testing their equipment (GLD was created in the US, indeed), and test conditions are defined there through T^{in}_{evap} and T^{in}_{cond}, in contrast to EN14511, which is the standard adopted mostly by European companies. Therefore, this fact further justifies the need for including the T^{in}_{cond} column in Table 1.

The GLD simulates the seasonal performance of the installation and provides a value for SCOP and SEER using the same system boundaries as those defined in expressions [3] and [4], so the simulation results are perfectly comparable o the ones measured.

Table 3 shows a comparison between the measured SCOP and SEER for the period going from April 2017 to March 2018 and the simulated values obtained by GLD for the same period and thermal loads, taking into consideration that the heat pump equipment would be operating according to the declared performance defined by Table 1.

Table 3. Measured and simulated SCOP and SEER corresponding to the period from April 2017 to March 2018, comprising two complete warm and cool seasons.

E_h+E_{DHW} (kWh)	E_c (kWh)	SCOP /SEER measured	SCOP /SEER simulated
85457		3.11	3.3
	40026	2.89	3.5

4. DISCUSSION

Although it is observed a clear decrease of EER and COP over the years, this is not correlated with the ground temperature evolution, so any change in T^{in}_{brine} must be discarded as a possible cause. Simulated SCOP and SEER values are greater than those measured for the same period of time, but closer to the values corresponding to the oldest period of observation in Table 2. This fact supports the idea that a progressive degradation could have been taking place since the commissioning of the SGE installation, although not necessarily following the linear trend shown in Figure 1. Besides, it is observed a significantly higher decay rate in EER than COP. This is attributed to the fact that $t^A_{ON}>t^B_{ON}$, especially during the warm season (take day plots Figure 4 as representative) since compressor A acts as the "master" unit and compressor B acts as the "slave" one, which means that compressor B only operates under high load conditions and therefore compressor A would be aging faster. Nevertheless, this "aging rate" is too high to be considered as regular aging (the SGE installation is only 6 years old), so other factors that are still unknown must come into play.

The representation of PLF(PLR) offers a significant picture of how part-load operation can affect the installation performance. However, the values obtained cannot be taken as a reliable quantification of the efficiency losses due to cycling operation regimes. There are several important factors and limitations in the methodology that are at least worth to mention. Firstly, the declared performance data shown in Table 1 is referred to the heat pump equipment, while the SGE installation as a whole shows several differences. Some elements concerning tests at the factory (brine composition, working flows at evaporator and condenser) differ from actual operating conditions. Moreover, rated performance of a specific heat pump unit admits a deviation margin compared to the declared performance stated by the manufacturer as such. Norm EN14511 specifies a tolerance in capacity testing up to 12% and up to 15% in EER / COP testing with respect to declared values.

Concerning T^{in}_{brine}, Figure 4 shows that when no heat is being supplied or removed from the building, T^{in}_{brine} is not a reliable readout. In theory T^{in}_{brine} must equal T^{out}_{brine} when the heat pump is not operative, but this is not observed, so averaged values of ON and OFF periods will yield non-representative values of average T^{in}_{brine}. Therefore, WA data concerning T^{in}_{brine} should be discarded in this particular case.

5. CONCLUSIONS

Remote monitoring of SGE installations and data processing offer an attractive tool for the characterisation of their performance. The quality and utility of the data depends on the time resolution employed for data collection. WA data is the best option in order to observe the evolution of COP and EER throughout large periods of time (years), as well as the ground temperature (through T^{out}_{brine}). MR data is preferred when identification or even quantification of efficiency losses due to part-load operation are pursued (based on the relationship between PLR and PLF). MR data is also necessary when lower time resolution can distort the accuracy in parameter measurement through averaging (like in the case of T^{in}_{brine}). 30MA (or 1 hour resolution, in general) is a useful time-scale in order to estimate building loads, but also to identify time periods with quasi steady conditions, which is mandatory in order to obtain consistent results from the PLF(PLR) analysis.

Concerning the particular case under study, the PLF(PLR) analysis evidences a correlation between system performance and part-load operation, showing differences in PLF greater than 10% between scenarios with low (PLR→0) and high (PLR→1) building loads. On the other side, it cannot be concluded from the PLF(PLR) analysis alone that the SGE installation shows a significant reduced capacity with respect to the declared values stated by the heat pump manufacturer. Nevertheless, WA data demonstrate that there exists a progressive decay in COP and EER since the beginning of data collection. Simulated SEER and SCOP support the observations. Although the reasons are still

unknown, this decrease cannot be attributed to a change in ground temperature.

The recorded parameters listed in section 2.2 allow a detailed analysis of an in-service SGE installation, but the processing methodology would be simpler and the analysis even fruitful if only a few more parameters were recorded systematically, namely: $\dot{V}_{evap}$, $\dot{V}_{cond}$, T_{evap}^{in}, T_{cond}^{in}, T_{evap}^{out}, T_{cond}^{out} and $T_{ambient}$.

REFERENCES

Corberán J.M., Donadello D., Martínez-Galván I., Montagud C., Partialization losses of ON/OFF operation of water-to-water refrigeration/heat-pump units, Int. J. Refrig. 36 (2013) 2251–2261.

EN 15316-4-2, Energy performance of buildings - Method for calculation of system energy requirements and system efficiencies - Part 4-2: Space heating generation systems, heat pump systems. CEN, Brussels (2017)

EN 14511, Air conditioners, liquid chilling packages and heat pumps with electrically driven compressors for space heating and cooling (2008)

EN 14825. Air Conditioners, Liquid Chilling Packages and Heat Pumps, with Electrically Driven Compressors, for Space Heating and Cooling d Testing and Rating at Part Load Conditions and Calculation of Seasonal Performance (2010).

EN 255, Air conditioners, liquid chilling packages and heat pumps with electrically driven compressors. Heating mode (1998).

Gehlin S., Spitler J. D., Larsson A. and Annsberg A.: Measured performance of the University of Stockholm Studenthuset ground source heat pump system, 14th International Conference on Energy Storage 25-28 April, Adana, TURKEY (2018)

Hughes D.: Monitoring of Non-Domestic Renewable Heat Incentive Ground-Source and Water-Source Heat Pumps, Report prepared for the Department for Business, Energy and Industrial Strategy from the UK Government (February 2018) (https://assets.publishing.service.gov.uk/government/uploads/system/uploads/attachment_data/file/680470/non-dom-rhi-heat-pumps-final-report.pdf)

ISO 13256, Water-source heat pumps. Testing and rating for performance (1998).

Miara M., Günther D., Langner R., Helmling S., Wapler J.: 10 years of heat pumps monitoring in Germany. Outcomes of several monitoring campaigns. From low-energy houses to unretrofitted single-family dwellings, 12th IEA Heat Pump Conference (2017), K.1.5.1

Nordman R., Andersson K., Axell M., Lindahl M., Calculation methods for SPF for heat pump systems for comparison, system choice and dimensioning, SP Report 2010:49. SP Technical Research Institute of Sweden (2010) (https://www.researchgate.net/publication/264880506_Calculation_methods_for_SPF_for_heat_pump_systems_for_comparison_system_choice_and_dimensioning)

Nordman R., Kleefkens O., Riviere P., Nowak T., Zottl A., Arzano-Daurelle C., Lehmann A., Polyzou O. , Karytsas K., Riederer P., Miara M., Lindahl M., Andersson K. and Olsson M.: SEPEMO-Build Project Final Report, (July 2012) (https://ec.europa.eu/energy/intelligent/projects/sites/iee-projects/files/projects/documents/sepemo-build_final_report_sepemo_build_en.pdf)

Office of Gas and Electricity Markets (OFGEM): The Domestic Renewable Heat Incentive (United Kingdom, 2014) (https://www.ofgem.gov.uk/environmental-programmes/domestic-rhi/about-domestic-rhi)

Office of Gas and Electricity Markets (OFGEM): Essential Guide to Metering and Monitoring Service Packages (United Kingdom, 2019) (https://www.ofgem.gov.uk/publications-and-updates/essential-guide-metering-and-monitoring-service-packages-mmsp)

Rolando D. and Madani H., Smart Control Strategies for Heat Pump Systems, Final Report of Project effsys-expand (Accessed online on the 19th of Feb-2019,)

Sparn B., Earle L., Christensen D., Maguire J. and Wilson E. and Hancock C.E.: Field Monitoring Protocol: Heat Pump Water Heaters, Technical Report from the National Renewable Energy Laboratory (United States) (February 2013) (https://www.nrel.gov/docs/fy13osti/57698.pdf)

Thermal dynamics Inc., Ground loop design, version 2016.

Waddicor D.A., Fuentes E., Azar M., Salom J., Partial load efficiency degradation of a water-to-water heat pump under fixed set-point control, Appl. Therm. Eng. 106 (2016) 275–285.

ACKNOWLEDGEMENTS

This work was supported by a grant from the Institut Cartogràfic i Geològic de Catalunya (ICGC) in the framework of the general research line on shallow geothermal energy.